



Corneal epithelial thickness mapping using Fourier-domain optical coherence tomography for detection of form fruste keratoconus

Cyril Temstet, MD, Otman Sandali, MD, Nacim Bouheraoua, MD, Taous Hamiche, Optm, Alice Galan, Optm, Mohamed El Sanharawi, MD, Elena Basli, MD, PhD, Laurent Laroche, MD, Vincent Borderie, MD, PhD

PURPOSE: To determine whether optical coherence tomography (OCT) epithelial mapping can improve the detection of form fruste keratoconus.

SETTING: French National Eye Hospital, Paris 6 Pierre & Marie Curie University, Paris, France.

DESIGN: Retrospective comparative study.

METHODS: Eyes with normal corneas, form fruste keratoconus, moderate keratoconus, or severe keratoconus were assessed using Fourier-domain OCT (RTVue 5.5), scanning-slit corneal topography (Orbscan IIz), and rotating Scheimpflug camera (Pentacam Comprehensive Eye Scanner). Several parameters provided by the software or derived from elevation maps, OCT pachymetric maps, and OCT epithelium parameters were evaluated and compared between the 4 groups.

RESULTS: The study involved 145 eyes. There were no significant differences in the keratometry (K) value, inferior–superior value, keratoconus index, central K index, and topographic keratoconus classification indices between the form fruste keratoconus group and the control group ($P > .05$). Form fruste keratoconic corneas had less epithelial thickness in the thinnest corneal zone than normal corneas, and greater epithelial thickness in the thinnest corneal zone than keratoconic corneas ($P < .005$). The epithelial thickness in the thinnest corneal zone in form fruste corneas was located inferiorly ($P < .005$) and corresponded with the zone of minimum epithelial thickness and maximum posterior elevation ($P < .005$). The receiver operating characteristic curve analysis showed good overall predictive accuracy of the epithelial thickness in the thinnest corneal zone, with a 52 μm threshold value for discriminating form fruste keratoconic corneas from normal corneas.

CONCLUSIONS: The epithelial thickness in the thinnest corneal zone and its location provided by the OCT epithelial mapping might be useful for the early diagnosis of form fruste keratoconus.

Financial Disclosure: No author has a financial or proprietary interest in any material or method mentioned.

J Cataract Refract Surg 2015; 41:812–820 © 2015 ASCRS and ESCRS

Keratoconus is a bilateral progressive corneal disease characterized by localized conical protrusion, apical thinning, irregular astigmatism, and central scarring. The reported incidence of keratoconus is much higher among candidates for refractive surgery than among the general population.¹ Accurate preoperative detection of keratoconus in refractive surgery

candidates is crucial because refractive surgery is contraindicated in these patients.^{1,2}

Form fruste keratoconus is the main cause of post-operative corneal ectasia after laser in situ keratomileusis.¹ However, the early stages of keratoconus are not easy to diagnose because these eyes frequently have normal clinical findings.^{1–3}

Many efforts have been made to recognize keratoconus in its earliest stages.⁴⁻¹⁹ Holland et al.²⁰ studied the incidence of unilateral topographic findings and corneal topography in keratoconus cases with unilateral topographic findings. They concluded that if observed long enough, most patients will develop the disease in the fellow eye. Li et al.²¹ prospectively observed 116 patients with clinical keratoconus with unilateral topographic findings and reported that approximately 50% of clinically normal fellow eyes progressed to keratoconus within 16 years. Therefore, an apparently normal fellow eye in keratoconus cases with unilateral topographic findings may be considered the ideal model of form fruste keratoconus for evaluating screening modalities.

The term *form fruste keratoconus*, first proposed by Amsler,²² should be used to define the contralateral eye in unilateral keratoconus, the form fruste being an incomplete, abortive, or unusual form of a syndrome or disease.¹³ The issue of false negatives in corneal topography has prompted extensive research to develop new tests for the detection of keratoconus that are more sensitive and mostly are developed from the tomographic analysis of the cornea. These include scanning-slit corneal topography, rotating Scheimpflug cameras, and very-high-frequency (VHF) digital ultrasound (US) arc scanning.

Reinstein et al.⁷ suggested that in very early keratoconus, epithelial compensation could mask the presence of an underlying cone on front-surface topography and a diagnosis of keratoconus might be missed by the use of topography alone. Significant central and regional epithelial thickness profile differences between keratoconic eyes, ectatic eyes, and control eyes were shown using spectral-domain optical coherence tomography (SD-OCT), with ectatic eyes showing significant variability and unpredictability.^{23,24} We are unaware of a published study

using OCT epithelial parameters to screen for form fruste keratoconus.

To determine whether OCT epithelial mapping can improve detection of form fruste keratoconus, the present study compared eyes with form fruste keratoconus with eyes with normal corneas and eyes with keratoconus that have positive topographic indices.

PATIENTS AND METHODS

This retrospective comparative study included eyes with mild to advanced keratoconus or form fruste keratoconus and eyes with normal corneas. All eyes were assessed using scanning-slit corneal topography (Orbscan IIz, Bausch & Lomb), a rotating Scheimpflug camera (Pentacam Comprehensive Eye Scanner, Oculus Optikgeräte GmbH), and Fourier-domain OCT (RTVue, Optovue, Inc.).

Keratoconus was diagnosed if all of these criteria were found: (1) keratoconic appearance on the topography map (asymmetric bow tie with skewed radial axis, central or inferior steep zone, or claw shape); (2) positive topographic indices on scanning-slit corneal topography assessment (mean keratometry [K] >47.0 diopters [D] or inferior-superior value [I-S] >1.4 D in the central 3.0 mm, according to Rabinowitz and McDonnell criteria⁶); (3) positive rotating Scheimpflug camera assessment (1 or more of a central keratometry index [CKI] >1.03, a keratometry index [KI] >1.07, and a positive topographic keratoconus classification)¹⁷; and (4) at least 1 clinical sign. A corneal specialist evaluated the slitlamp findings for Munson sign, Vogt striae, Fleischer ring, apical thinning, Rizutti sign, and corneal scarring consistent with keratoconus. The distinction between moderate and severe keratoconus was based on the rotating Scheimpflug camera's topographic keratoconus classification,¹⁷ with moderate keratoconus corresponding to grades I and II and severe keratoconus to grades III and IV.

Form fruste keratoconus was diagnosed if all these criteria were found: (1) normal topography; (2) negative scanning-slit corneal topography indices ($K \leq 47.0$ D and $I-S \leq 1.4$); (3) negative rotating Scheimpflug camera indices ($KI < 1.03$, $CKI < 1.07$, and a negative topographic keratoconus classification); (4) a normal slitlamp examination; and (5) keratoconus in the fellow eye. Eyes in the control group were selected from a database of consecutive candidates for refractive surgery and met the following criteria: (1) normal topography; (2) negative scanning-slit corneal topography indices ($K \leq 47.0$ D and $I-S \leq 1.4$); (3) negative rotating Scheimpflug device indices ($KI < 1.03$, $CKI < 1.07$, and negative topographic keratoconus classification); (4) a normal slitlamp examination; and (5) no history of eye disease.

Exclusion criteria included previous ocular surgery or trauma; associated corneal pathologic features; a history of collagen crosslinking, intrastromal corneal ring segment implantation, keratoplasty, or other corneal surgery; and contact lens wear during the previous 3 weeks. One eye of each patient was included in the study.

For patients with bilateral keratoconus and the control group eyes, the study eye was selected using a random-number table. In accordance with French law, institutional review board and ethics committee approval were not required for this study because no modifications to French standards of treatment or follow-up were made. All patients

Submitted: September 17, 2013.

Final revision submitted: June 13, 2014.

Accepted: June 17, 2014.

From Centre Hospitalier National d'Ophtalmologie des XV-XX (Temstet, Sandali, Bouheraoua, Hamiche, Galan, El Sanharawi, Basli, Laroche, Borderie), Pierre et Marie Curie University, and Research Team 968 (Bouheraoua, Laroche, Borderie), Institut de la Vision, Paris, France.

Supported by University Pierre et Marie Curie-Paris 6, Paris, France.

Corresponding author: Cyril Temstet, MD, Centre Hospitalier National d'Ophtalmologie des XV-XX, 28 rue de Charenton, 75571 Paris, France. E-mail: ctemstet@gmail.com.

gave written informed consent. All procedures followed the tenets of the Declaration of Helsinki.

A 26 000 Hz Fourier-domain OCT system with a 5 μm axial resolution was used with a corneal adaptor module. The system works at an 830 nm wavelength and has a scan speed of 26 000 axial scans per second. The depth resolution is 5 μm (full-width half-maximum) in tissue. The wide-angle (corneal long) adaptor lens used in this study provided a 6.0 mm scan width with a transverse resolution of 15 μm (focused spot size). The cornea was mapped using a Pachymetry + Cpwr scan pattern (6.0 mm scan diameter, 8 radials, 1024 axial scans each, and 5 repetitions) centered on the middle of the pupil. The corneal adaptor module software (software version 5.5) automatically processed the OCT scan to provide the pachymetry (corneal-thickness) and the epithelial-thickness maps.

Commercial software of epithelial mapping²⁵ was used to calculate the following corneal-thickness and epithelial-thickness parameters: minimum corneal thickness, superonasal-inferotemporal (SN-IT) corneal thickness, I-S corneal thickness, minimum-median (min-med) corneal thickness, I-S epithelial thickness, thinnest epithelial thickness, minimum-maximum (min-max) epithelial thickness, and the standard deviation (SD) of the epithelial thickness.

All calculations were performed within the 5.0 mm central zone of the cornea, with the cornea divided into quadrants: inferotemporal (IT), inferonasal (IN), superotemporal (ST), and superonasal (SN). The localization of the thinnest corneal point, the thinnest epithelial point, and the epithelial thickness in the thinnest corneal zone were also recorded. The epithelial thickness in the thinnest corneal zone was obtained automatically by pointing the mouse to the thinnest corneal zone on the pachymetry map and recording the corresponding epithelial thickness in the thinnest corneal zone. The maximum posterior corneal elevation was also recorded using the rotating Scheimpflug imaging system.

Each examination was performed by 2 experienced operators (T.H., A.G.). At least 2 images were obtained of each eye to ensure reproducibility of the video and OCT images. The images were visually inspected and the best selected according to the quality of the keratoscope photographs and OCT scans. The quantitative variables were analyzed using 1-way analysis of variance with post hoc tests. A Bonferroni correction was used to control type I error. Receiver operating characteristic (ROC) curves were used to determine the overall predictive accuracy of the significant test parameters as described by the area under the curve (AUC) and to calculate the sensitivity and specificity of the parameters. These curves were obtained by plotting sensitivity against 1-specificity, calculated for each value observed. This approach also was used to calculate specificity, sensitivity, and positive (sensitivity/[1-specificity]) and negative ([1-sensitivity]/specificity) likelihood ratios (LRs) for cutoff points.⁸ Qualitative variables were analyzed using the Fisher test.

For all analyses, a *P* value less than 0.05 was considered statistically significant.

RESULTS

The study assessed 145 eyes of 103 patients and 42 subjects from December 2, 2012, to May 27, 2013. The moderate keratoconus group included 35 eyes of 35 patients (mean age 29.3 years \pm 7.6 [SD]). The severe keratoconus group included 32 eyes of 32 patients

(mean age 29.9 \pm 8.9 years). The form fruste keratoconus group included 36 eyes of 36 patients (mean age 28.9 \pm 9.9 years). The control group included 42 eyes with normal corneas of 42 subjects (mean age 36.1 \pm 9.4 years). There were no significant differences in age distribution between the 4 groups (*P* > .05). Table 1 shows the mean values of all parameters evaluated in the 4 groups. The differences between the moderate and severe keratoconus groups and the control group were statistically significant for all parameters (*P* < .001).

The mean epithelial thickness in the thinnest corneal zone was statistically significantly less in the form fruste keratoconus group (49.7 \pm 2.9 μm) than in the control group (53.4 \pm 3.3 μm) (*P* < .005) (Figure 1) and greater than in the keratoconus groups (*P* < .005) (Figure 1). For all other corneal- and epithelial-thickness parameters, there were no statistically significant differences between the form fruste keratoconus group and the control group (*P* > .05) except for the minimum corneal thickness, which was lower in the form fruste group (*P* < .005) (Table 1).

Figure 2 shows the ROC curve of the epithelial thickness in the thinnest corneal zone. A positive test result corresponds to form fruste keratoconus and a negative test result to normal corneas. The ROC graph (Figure 3) shows that the epithelial thickness in the thinnest corneal zone differentiates form fruste keratoconic corneas from normal corneas. The optimum cutoff point to identify eyes with form fruste keratoconus is estimated to be 52 μm . This threshold value is associated with an 88.9% sensitivity (95% confidence interval [CI], 73.9%-96.1%) and a 59.5% specificity (95% CI, 44.5%-72.9%), a positive likelihood ratio of 2.196, a negative likelihood ratio of 0.187, a positive predictive value of 0.653, and negative predictive value of 0.862.

The thinnest point of the cornea was in the IT quadrant in the form fruste keratoconus group (20 eyes; 55.5%) and in the control group (21 eyes; 50.0%) without statistically significant difference (*P* = .6) (Table 2). The thinnest epithelial point corresponded with the thinnest corneal point in 33 eyes (91.6%) with form fruste keratoconus (*P* < .005) and was located inferiorly (Tables 2 to 4). In the control group, the thinnest epithelial point more often was located superiorly (30 eyes; 71.4%) and temporally (18 eyes; 42.9%) (*P* < .005) (Table 3). The maximum posterior corneal elevation point (10.5 \pm 4.0 μm) corresponded to the zone minimum corneal point in form fruste keratoconus (100%) and was statistically significantly higher than the control group corneas (mean 3.6 \pm 2.2 μm) (*P* < .05) (Table 1).

Figure 4 shows the ROC curve of the maximum posterior corneal elevation. A positive test result

Table 1. Comparison of the mean values in the 4 study groups.

Parameter	Group				P Value	
	Form Fruste Keratoconus	Moderate Keratoconus	Severe Keratoconus	Control	ANOVA	Form Fruste vs Control
Keratometry (D)						
K	43.1 ± 1.5	45.5 ± 2.6	49.7 ± 3.5	43.2 ± 1.3	< .001	.997
I-S	0.5 ± 0.6	4.2 ± 4.5	10.0 ± 3.9	0.07 ± 0.4	< .001	.879
KI	1.02 ± 0.02	1.09 ± 0.06	1.39 ± 0.12	1.01 ± 0.02	< .001	.762
CKI	1.00 ± 0.01	1.03 ± 0.03	1.12 ± 0.03	0.99 ± 0.01	< .001	.998
Epithelial thickness (µm)						
Min	48.3 ± 3.6	42.8 ± 5.4	35.4 ± 9.2	49.1 ± 3.1	< .001	.947
Min-Max	-7.9 ± 3.5	-18.1 ± 10.8	-30.9 ± 13.2	-6.5 ± 2.1	< .001	.105
SN-IT	-0.5 ± 2.7	1.8 ± 5.5	7.1 ± 5.6	-2.7 ± 1.7	< .001	.891
SD	1.8 ± 0.8	4.6 ± 2.7	7.6 ± 3.0	1.4 ± 0.7	< .001	.830
Central	52.8 ± 3.3	49.5 ± 5.2	47.9 ± 4.9	53.0 ± 3.1	< .001	.961
Corneal zone (µm)						
Thinnest	49.7 ± 2.9	46.6 ± 5.4	46.3 ± 6.4	53.4 ± 3.3	< .001	.003
Max posterior elevation	10.5 ± 4.0	40.9 ± 11.0	50.3 ± 10.9	7.0 ± 2.2	< .001	.003
Min thickness	500.8 ± 34.2	447.4 ± 46.1	403.9 ± 44.2	542.0 ± 31.4	< .001	< .001
Min-med thickness	-26.2 ± 7.2	-39.3 ± 22.3	-69.1 ± 19.6	-21.2 ± 3.7	< .001	.483
I-S thickness	-27.2 ± 13.0	-39.1 ± 26.1	-55.4 ± 35.5	-18.6 ± 11.3	< .001	.385
SN-IT thickness	-32.2 ± 16.5	-52.3 ± 23.1	-63.7 ± 34.2	-25.7 ± 11.8	< .001	.203

ANOVA = analysis of variance; CKI = central keratometry index; K = keratometry; KI = keratometry index; I-S = inferior-superior value; max = maximum; min = minimum; min-med = minimum-median; OCT = optical coherence tomography; SD = standard deviation; SN-IT = superonasal-inferotemporal

corresponds to form fruste keratoconus and a negative test result to normal corneas. The ROC graph shows that the maximum posterior corneal elevation differentiates form fruste keratoconic corneas from normal corneas (Figure 5). The optimum cutoff point to identify eyes with form fruste keratoconus is estimated to be 8 µm. This cutoff point is associated with a 72.2% sensitivity (95% CI, 55.8%-84.2%) and an 83.3 % specificity (95% CI, 69%-91.9%), a positive likelihood ratio of 4.333, a negative likelihood ratio of 0.333, a positive

predictive value of 0.788, and a negative predictive value of 0.778.

Using logistic regression analysis, cutoff points were similar to those identified by ROC analysis. In comparing form fruste keratoconus and normal eyes, the model fit well with the data and the data changed only marginally after validation using bootstrap analysis.

DISCUSSION

In this series, we studied the epithelial thickness profile of form fruste keratoconus. Our findings might improve the detection of the form fruste keratoconus and will be combined with curvature, aberrometric, and biomechanical corneal parameters.

Other studies have defined form fruste keratoconus as clinically unilateral keratoconus²¹ or, in 1 case,¹³ according to neural network criteria. In the present study, the study group was selected using objective parameters: Scheimpflug rotating camera classification and 2 variables (KI and CKI) that were reported to be good parameters for differentiating subclinical keratoconic eyes from normal eyes.¹⁷ All the topographic indices, including K, I-S value, KI, CKI, and the topographic keratoconus classification, were normal in the form fruste keratoconus group in this study.

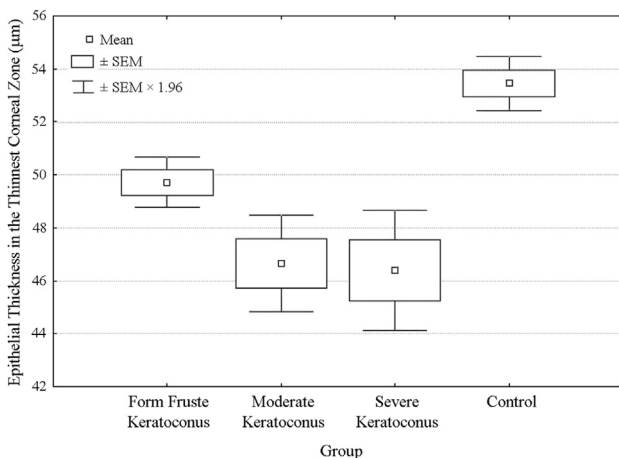


Figure 1. Epithelial thickness in the thinnest corneal zone in the 4 groups of eyes (SEM = standard error of the mean).

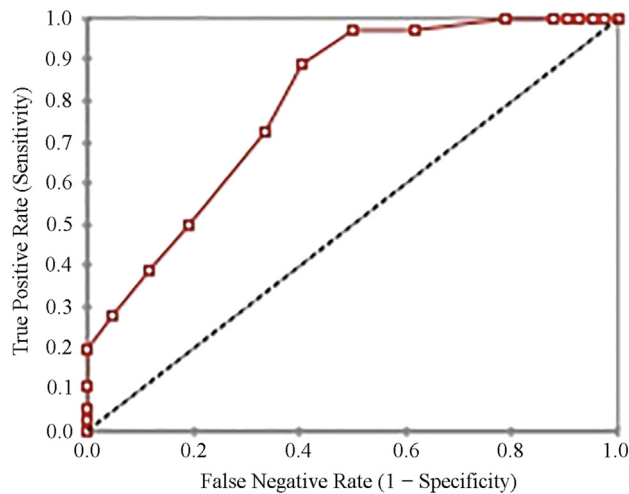


Figure 2. The ROC curve for the epithelial thickness in the thinnest corneal zone. The area under the curve is 0.795 μ m.

Reinstein et al.^{7,26,27} pioneered the use of corneal epithelial mapping using VHF US (50 MHz) with a 21 μ m resolution over the entire corneal surface. They performed a 3-dimensional epithelial thickness analysis for the central 8.0 to 10.0 mm diameter in normal eyes and in keratoconic eyes. The central epithelial thickness in normal eyes in that study was $53.4 \pm 4.6 \mu$ m.²⁷ In keratoconic eyes, the corneal epithelium showed an epithelial doughnut pattern characterized by localized central thinning surrounded by an annulus of thick epithelium, and the central epithelial thickness ($45.7 \pm 5.9 \mu$ m) was statistically significantly thinner than in normal eyes.^{7,26}

Anterior segment OCT has been used to measure the epithelial layer in normal eyes and keratoconic eyes.^{23,28,29} Using time-domain OCT, Haque et al.²⁸ reported a central corneal epithelial thickness of 54.7 μ m in normal eyes. They also showed that the central epithelial thickness in keratoconic eyes was thinner than in normal eyes (a 4.7 μ m average difference). Rocha et al.²³ described a regional epithelial thickness profile in keratoconic eyes, eyes with postoperative ectasia, and normal eyes. They found that the mean epithelial thickness at the highest point in the meridian was statistically significantly thinner in eyes with keratoconus ($P < .0001$) and ectasia ($P = .0007$) than in normal eyes, calculated as $41.18 \pm 6.47 \mu$ m, $46.5 \pm 6.72 \mu$ m, and $50.45 \pm 3.92 \mu$ m, respectively.

Rocha et al.²³ analyzed regional epithelial thickness profiles in keratoconic eyes, eyes with postoperative corneal ectasia, and normal eyes and reported that total cornea thickness is not predictive of localized regions of stromal thinning or epithelial thickening. We agree with respect to keratoconus cases; however,

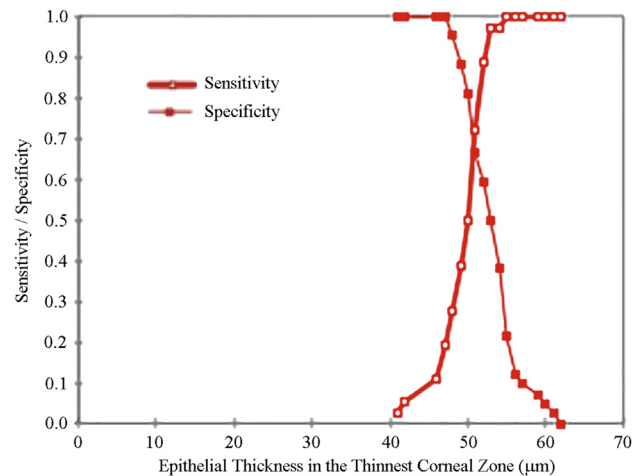


Figure 3. The ROC graph of the epithelial thickness in the thinnest corneal zone.

we did not observe epithelial thickening in form fruste keratoconic eyes. In our study, the area of epithelial thinning corresponded to the area of the steepest corneal curvature, highest elevation, and thinnest point ($P < .05$).

We used epithelial-mapping software with Fourier-domain OCT developed by Li et al.²⁹ to determine the characteristics of the epithelium in keratoconic eyes. Their study²⁹ found no statistically significant difference in the central epithelial thickness between keratoconic and normal corneas but did find the SI, min-max epithelial thickness differences, and SD to be higher. The differences between these indices were also statistically significant between the moderate keratoconus and severe keratoconus groups and the control group in our study ($P < .001$).

To our knowledge, there are no published studies using OCT epithelial parameters to screen for form fruste keratoconus; thus, we cannot compare our results with those in others studies. When comparing these parameters in the form fruste keratoconus group and the control group, we found no statistically significant differences. However, the epithelial thickness of the thinnest corneal point and its location were statistically significant between the form fruste keratoconus group and the control group. In our series, the thinnest epithelial point was located inferiorly in 33 (91.3%) of the form fruste keratoconus eyes compared with the normal (control) corneas, which corresponded to the location of the thinnest point on pachymetry in form fruste keratoconic eyes. Moreover, the form fruste keratoconic corneas featured statistically significantly lower epithelial thickness at the thinnest corneal zone than the control group corneas and higher epithelial thickness at the thinnest corneal zone than the keratoconic corneas ($P < .005$), with a 52 μ m

Table 2. Location of the thinnest point of cornea in the 4 groups (N = 145).

Group	Location			
	Inferotemporal	Inferonasal	Superotemporal	Superonasal
Form fruste keratoconus				
Eyes (n)	20	16	0	0
Eyes (%)	55.5	45.5	0	0
Moderate keratoconus				
Eyes (n)	28	7	0	0
Eyes (%)	80.0	20.0	0	0
Severe keratoconus				
Eyes (n)	29	3	0	0
Eyes (%)	90.6	9.4	0	0
Control				
Eyes (n)	21	18	2	1
Eyes (%)	50.0	42.9	4.7	2.4

threshold value. These 2 parameters might improve the detection of form fruste keratoconus.

Reinstein et al.²⁷ used VHF US to locate the thinnest epithelial point in normal corneas, which is located in the ST quadrant. To clarify, this applied to the mean location of the thinnest epithelial point, although the SDs were very large in the x (± 1.08 mm) and y (± 0.96 mm) directions; therefore, the thinnest epithelial point was not in the ST quadrant in all eyes.

We determined the thinnest epithelial point to be in the ST quadrant in the control group (18 eyes; 42.8%) and found a statistically significant difference in the location of the thinnest epithelial point between form fruste keratoconic eyes and control eyes, which was inferiorly in form fruste keratoconus (34 eyes; 92.4%) ($P < .005$). Reinstein et al.²⁶ used VHF US to determine the location of the thinnest epithelial point in the IT quadrant for keratoconus. Interestingly, the results in

our study were similar even though our OCT scans centered on the center of the pupil,²⁵ which was not displaced by the cone location, rather than on the corneal vertex, as with the VHF US map. The epithelial doughnut pattern of a thickened epithelium surrounding the thin epithelial zone at the cone as described by Reinstein et al.²⁷ was not found in the form fruste keratoconus group in our study. This profile will appear in keratoconus and corresponds to stage 1 in our OCT keratoconus classification.³⁰ In the keratoconus in Reinstein et al.,²⁶ because the cone was protruding, the apex would have been the first point of contact with the eyelid, resulting in increased chafing and therefore thinning of the epithelium at the apex of the cone.

Regarding the corneal thickness, Li et al.²⁵ showed that OCT pachymetry maps accurately detect the characteristics of abnormal corneal thinning in keratoconic

Table 3. Location of the thinnest epithelial point in the 4 groups (N = 145).

Group	Location			
	Inferotemporal	Inferonasal	Superotemporal	Superonasal
Form fruste keratoconus				
Eyes (n)	24	10	1	1
Eyes (%)	66.6	27.8	2.8	2.8
Moderate keratoconus				
Eyes (n)	26	9	0	0
Eyes (%)	74.3	25.7	0	0
Severe keratoconus				
Eyes (n)	27	5	0	0
Eyes (%)	84.4	15.6	0	0
Control				
Eyes (n)	7	5	18	12
Eyes (%)	16.6	11.9	42.8	28.7

Table 4. Correspondence between minimum epithelial thickness, minimum corneal thickness, and maximum posterior corneal elevation.

Group	Location			
	Inferotemporal	Inferonasal	Superotemporal	Superonasal
All same point				
Eyes (n)	33	33	19	10
Eyes (%)	91.6	94.3	59.4	23.8
Different points				
Eyes (n)	3	2	13	32
Eyes (%)	8.4	5.7	40.6	76.2

eyes. They studied corneal thickness parameters from the OCT such as min-med, I-S, SN-IT, and minimum corneal thickness and found minimum corneal thickness to be the best parameter (ROC value 0.954) for differentiating keratoconic corneas from normal corneas. Central corneal thickness has been surpassed significantly by thickness progression analysis.¹⁶

Many studies describe the maximum posterior corneal elevation and suggest that it is an early sign of keratoconus—with limited sensitivity and specificity to differentiate between form fruste keratoconic eyes and normal eyes—as a single datum.^{8,9,13–15,31,32} The limitations of the present study include the low specificity and sensitivity of the epithelial thickness in the thinnest corneal zone cutoff value. Although it has been suggested that a decrease in epithelial thickness at the thinnest corneal zone might be the earliest sign of form fruste keratoconus, this value derives from a single datum. Another limitation of this study is that the interpretation of the epithelial thickness value is limited by the 5 μm resolution. It is important to clarify that the epithelial thickness measurements using SD-OCT include the tear film, whereas VHF

digital US measurements do not because they are performed using an immersion technique.

Reinstein et al.³³ reported, “The potential error of VHF digital ultrasound measurements is based upon the known speed of sound in cornea (1640 m/s) and the maximum theoretical limits of this speed of sound. ... Given these range limits for the speed of sound, a theoretical error analysis predicts an absolute maximum potential error of 1.8% for the accuracy of VHF digital ultrasound measurements.” An error of 1.8% translates to less than 1 μm ; therefore, VHF US-based epithelial measurements are closer to the true value than OCT measurements (which are made after assumptions about the refractive index of the epithelium versus the stroma³⁴). Also, because OCT measurements include the tear film as an additional variable, potential inaccuracies of the absolute values produced by OCT epithelial measurements are another limitation of the present study.

Topographic indices, which include multiple parameters and require integration of the data into a decision-making process such as a neural network, might be more sensitive and specific for distinguishing

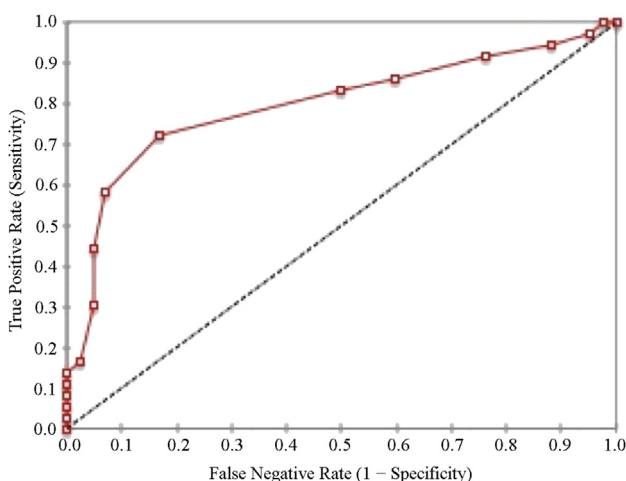


Figure 4. The ROC curve of the maximum corneal elevation. The area under the curve is 0.798 μm .

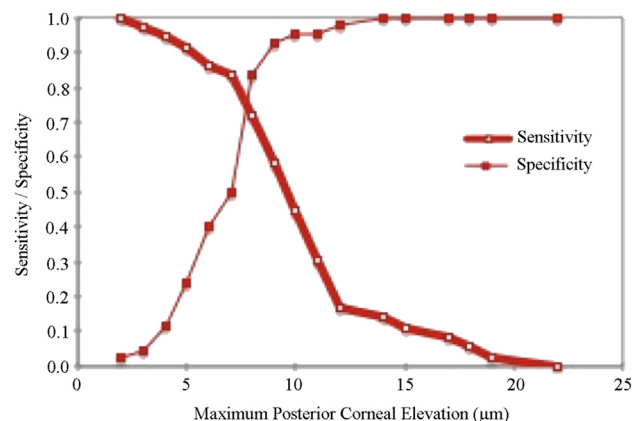


Figure 5. The ROC graph of the maximum posterior corneal elevation.

form fruste keratoconus.^{13,32,35} It would be valuable to include multiple OCT parameters, including the location and thickness of the thinnest epithelial point and to create an automated tree classification for a decision-making process.

In conclusion, using a corneal epithelial thickness profile analysis in the clinical setting might aid in the interpretation of corneal topography in keratoconic eyes and improve the detection of form fruste keratoconus. Spectral-domain OCT high-resolution cross-sectional scans showed significant differences in the epithelial thickness profiles in eyes with keratoconus and form fruste keratoconus compared with normal eyes. The epithelial thickness in the thinnest corneal zone and its location provided by the OCT epithelial mapping might be useful for early diagnosis of form fruste keratoconus. It cannot be concluded from this study whether epithelial thickness in the thinnest corneal zone is sufficient as a sole diagnostic index; however, this index does seem to be effective in differentiating form fruste keratoconic corneas from normal corneas, although the 52 μm cutoff point is debatable. Optical coherence tomography is commonly used in ophthalmologic practice and provides a very quick acquisition. Thus, data concerning epithelial thickness in the thinnest corneal zone should be combined with curvature, aberrometric, and biomechanical data in stratifying patients with form fruste keratoconus. Technological progress of OCT in the future should improve the accuracy value of the cutoff point of epithelial thickness in the thinnest corneal zone.

WHAT WAS KNOWN

- Optical coherence tomography parameters can be used to diagnose keratoconus.

WHAT THIS PAPER ADDS

- Epithelial thickness in the thinnest corneal zone and its location can be used to diagnose form fruste keratoconus, but is not sufficient as the sole diagnostic index.

REFERENCES

1. Randleman JB, Woodward M, Lynn MJ, Stulting RD. Risk assessment for ectasia after corneal refractive surgery. *Ophthalmology* 2008; 115:37–50
2. Binder PS. Risk factors for ectasia after LASIK [letter]. *J Cataract Refract Surg* 2008; 34:2010–2011
3. Klyce SD. Chasing the suspect: keratoconus [editorial]. *Br J Ophthalmol* 2009; 93:845–847
4. Maguire LJ, Bourne WM. Corneal topography of early keratoconus. *Am J Ophthalmol* 1989; 108:107–112
5. Maeda N, Klyce SD, Smolek MK. Comparison of methods for detecting keratoconus using videokeratography. *Arch Ophthalmol* 1995; 113:870–874
6. Rabinowitz YS, McDonnell PJ. Computer-assisted corneal topography in keratoconus. *Refract Corneal Surg* 1989; 5:400–408
7. Reinstein DZ, Archer TJ, Gobbe M. Corneal epithelial thickness profile in the diagnosis of keratoconus. *J Refract Surg* 2009; 25:604–610
8. de Sanctis U, Loiacono C, Richiardi L, Turco D, Mutani B, Grignolo FM. Sensitivity and specificity of posterior corneal elevation measured by Pentacam in discriminating keratoconus/subclinical keratoconus. *Ophthalmology* 2008; 115:1534–1539
9. Schlegel Z, Hoang-Xuan T, Gatinel D. Comparison of and correlation between anterior and posterior corneal elevation maps in normal eyes and keratoconus-suspect eyes. *J Cataract Refract Surg* 2008; 34:789–795
10. Bühren J, Kook D, Yoon G, Kohner T. Detection of subclinical keratoconus by using corneal anterior and posterior surface aberrations and thickness spatial profiles. *Invest Ophthalmol Vis Sci* 2010; 51:3424–3432. Available at: <http://www.iovs.org/content/51/7/3424.full.pdf>. Accessed November 16, 2014
11. Jafri B, Li X, Yang H, Rabinowitz YS. Higher order wavefront aberrations and topography in early and suspected keratoconus. *J Refract Surg* 2007; 23:774–781
12. Saad A, Gatinel D. Evaluation of total and corneal wavefront high order aberrations for the detection of forme fruste keratoconus. *Invest Ophthalmol Vis Sci* 2012; 53:2978–2992. Available at: <http://www.iovs.org/content/53/6/2978.full.pdf>. Accessed November 16, 2014
13. Saad A, Gatinel D. Topographic and tomographic properties of forme fruste keratoconus corneas. *Invest Ophthalmol Vis Sci* 2010; 51:5546–5555. Available at: <http://www.iovs.org/content/51/11/5546.full.pdf>. Accessed November 16, 2014
14. Saad A, Lteif Y, Azan E, Gatinel D. Biomechanical properties of keratoconus suspect eyes. *Invest Ophthalmol Vis Sci* 2010; 51:2912–2916. Available at: <http://www.iovs.org/content/51/6/2912.full.pdf>. Accessed November 16, 2014
15. Piñero DP, Alió JL, Alesón A, Escaf Vergara M, Miranda M. Corneal volume, pachymetry, and correlation of anterior and posterior corneal shape in subclinical and different stages of clinical keratoconus. *J Cataract Refract Surg* 2010; 36:814–825
16. Ambrósio R Jr, Alonso RS, Luz A, Coca Velarde LG. Corneal-thickness spatial profile and corneal-volume distribution: tomographic indices to detect keratoconus. *J Cataract Refract Surg* 2006; 32:1851–1859. Available at: http://www.ic.unicamp.br/~wainer/cursos/2s2008/ia/ambrosio_ct_profile.pdf. Accessed November 16, 2014
17. Uçakhan ÖÖ, Çetinkor V, Özkan M, Kanpolat A. Evaluation of Scheimpflug imaging parameters in subclinical keratoconus, keratoconus, and normal eyes. *J Cataract Refract Surg* 2011; 37:1116–1124
18. Rao SN, Raviv T, Majmudar PA, Epstein RJ. Role of Orbscan II in screening keratoconus suspects before refractive corneal surgery. *Ophthalmology* 2002; 109:1642–1646
19. Schweitzer C, Roberts CJ, Mahmoud AM, Colin J, Maurice-Tison S, Kerautret J. Screening of forme fruste keratoconus with the ocular response analyzer. *Invest Ophthalmol Vis Sci* 2010; 51:2403–2410. Available at: <http://www.iovs.org/content/51/5/2403.full.pdf>. Accessed November 16, 2014
20. Holland DR, Maeda N, Hannush SB, Riveroll LH, Green MT, Klyce SD, Wilson SE. Unilateral keratoconus. Incidence and quantitative topographic analysis. *Ophthalmology* 1997; 104:1409–1413
21. Li X, Rabinowitz YS, Rasheed K, Yang H. Longitudinal study of the normal eyes in unilateral keratoconus patients. *Ophthalmology* 2004; 111:440–446

22. Amsler M. Die "forme fruste" des Keratokonus [The "forme fruste" of keratoconus]. *Wien Klin Wochenschr* 1961; 73:842–843
23. Rocha KM, Perez-Straziota CE, Stulting RD, Randleman JB. SD-OCT analysis of regional epithelial thickness profiles in keratoconus, postoperative corneal ectasia, and normal eyes. *J Refract Surg* 2013; 29:173–179; errata, 234
24. Huang D, Tang M, Shekhar R. Mathematical model of corneal surface smoothing after laser refractive surgery. *Am J Ophthalmol* 2003; 135:267–278
25. Li Y, Meisler DM, Tang M, Lu ATH, Thakrar V, Reiser BJ, Huang D. Keratoconus diagnosis with optical coherence tomography pachymetry mapping. *Ophthalmology* 2008; 115:2159–2166
26. Reinstein DZ, Gobbe M, Archer TJ, Silverman RH, Coleman DJ. Epithelial, stromal, and total corneal thickness in keratoconus: three-dimensional display with Artemis very-high frequency digital ultrasound. *J Refract Surg* 2010; 26:259–271. Available at: <http://www.ncbi.nlm.nih.gov/pmc/articles/PMC3655809/pdf/nihms211821.pdf>. Accessed November 16, 2014
27. Reinstein DZ, Archer TJ, Gobbe M, Silverman RH, Coleman DJ. Epithelial thickness in the normal cornea: three-dimensional display with Artemis very high-frequency digital ultrasound. *J Refract Surg* 2008; 24:571–581. Available at: <http://www.ncbi.nlm.nih.gov/pmc/articles/PMC2592549/pdf/nihms78856.pdf>. Accessed November 16, 2014
28. Haque S, Jones L, Simpson T. Thickness mapping of the cornea and epithelium using optical coherence tomography. *Optom Vis Sci* 2008; 85:E963–E976. Available at: http://journals.lww.com/optvissci/Fulltext/2008/10000/Contrast_Sensitivity_Function_in_Patients_with.14.aspx. Accessed November 16, 2014
29. Li Y, Tan O, Brass R, Weiss JL, Huang D. Corneal epithelial thickness mapping by Fourier-domain optical coherence tomography in normal and keratoconic eyes. *Ophthalmology* 2012; 119:2425–2433. Available at: <http://www.ncbi.nlm.nih.gov/pmc/articles/PMC3514625/pdf/nihms389040.pdf>. Accessed November 16, 2014
30. Sandali O, El Sanharawi M, Temstet C, Hamiche T, Galan A, Ghoulali W, Goemaere I, Basli E, Borderie V, Laroche L. Four-domain optical coherence tomography imaging in keratoconus; a corneal structural classification. *Ophthalmology* 2013; 120:2403–2412
31. Muftuoglu O, Ayar O, Ozulken K, Ozyol E, Akýncý A. Posterior corneal elevation and back difference corneal elevation in diagnosing forme fruste keratoconus in the fellow eyes of unilateral keratoconus patients. *J Cataract Refract Surg* 2013; 39:1348–1357
32. Fukuda S, Beheregaray S, Hoshi S, Yamanari M, Lim Y, Hiraoka T, Yasuno Y, Oshika T. Comparison of three-dimensional optical coherence tomography and combining a rotating Scheimpflug camera with a Placido topography system for forme fruste keratoconus diagnosis. *Br J Ophthalmol* 2013; 97:1554–1559
33. Reinstein DZ, Archer TJ, Gobbe M, Silverman RH, Coleman DJ. Repeatability of layered corneal pachymetry with the Artemis very high frequency digital ultrasound arc-scanner. *J Refract Surg* 2010; 26:646–659. Available at: http://www.arcscan.com/news/reinstein_repeatability_cornea_layers_tprs_2008.pdf. Accessed November 16, 2014
34. Patel S, Marshall J, Fitzke FW III. Refractive index of the human corneal epithelium and stroma. *J Refract Surg* 1995; 11:100–105
35. Smadja D, Touboul D, Cohen A, Doveh E, Santhiago MR, Mello GR, Krueger RR, Colin J. Detection of subclinical keratoconus using an automated decision tree classification. *Am J Ophthalmol* 2013; 156:237–246



First author:
Cyril Temstet, MD

*Centre Hospitalier National
d'Ophthalmologie des XV-XX,
Paris, France*